Rare Metal Materials and Engineering
Volume 46, Issue 7, July 2017
Online English edition of the Chinese language journal

Available online at www.sciencedirect.com
ScienceDirect

Cite this article as: Rare Metal Materials and Engineering, 2017, 46(7): 1815-1820.

ARTICLE

Critical Conditions of Dynamic Recrystallization for B_4C_p/6061Al Composite

Liu Shengpu, Li Defu, Guo Shengli

General Research Institute of Non-ferrous Metals, Beijing100088, China

Abstract: Flow behavior and dynamic recrystallization (DRX) critical conditions of 25vol% B_4C_p/6061Al composite were investigated by isothermal compression tests at temperatures ranging from 350 to 500 ℃ with strain rates of 0.001 to 1 s^{-1}. The stress-strain curves show that DRX is the main softening mechanism of the composite, and an Arrhenius-type equation is developed using peak stress. Based on the strain hardening rate curves (θ-σ), the critical strain (ε_c) and critical stress (σ_c) are identified to express the initiation of DRX. The results indicate that there is a liner relationship between σ_c and σ_p:σ_c=0.8374σ_p–0.33708. The Zener-Hollomon parameter was also introduced to describe the effect of deformation conditions on critical conditions: $\varepsilon_c=2.39\times10^{-4}Z^{0.11022}$. In addition, the steady-state strains (ε_{ss}) were determined by the θ-ε curves, and then the DRX diagram was established.

Key words: B_4C_p/6061Al composite; dynamic recrystallization; critical conditions; strain hardening rate

B_4C particulate reinforced aluminum matrix composites have been rapidly developed over the past decades because of their excellent mechanical properties such as high strength, high wear resistance, high elastic modulus, good chemical stability, light weight and low thermal expansion coefficient[1,2]. Applications of B_4C_p/Al composites involve neutron absorber materials, armor plate materials and substrate material for computer hard disks[3-5]. However, compared with unreinforced alloys, particulately reinforced metal matrix composites are more sensitive to processing parameters including deformation temperature, strain rate and true strain. The interface between the reinforcements and matrix also plays an important role during the hot deformation process of composite, because the load is transferred from ductile matrix to brittle particles. Then the stress in the vicinity of non-deforming particles is difficult to be released and causes stress concentration, which lead to severe damages such as particles fracture and interface decohesion. As a result, the hot workability of composites is much worse than that of soft matrix.

Generally, the flow behavior of metals or alloys is very complex in the hot forming process. Strain hardening and dynamic softening (dynamic recovery and dynamic recrystallization) often occur simultaneously, which lead to annihilation and rearrangement of dislocations[6]. The dynamic recovery (DRV) begins at the initial stage of deformation and causes the accumulation of dislocation until the dislocation density reaches a critical value for inducing dynamic recrystallization (DRX)[7]. Critical conditions mainly depend on the chemical composition of the material, the grain size prior to deformation, mode of deformation and the deformation conditions[8]. DRX is not only a vital softening mechanism, but also an effective approach to control microstructure and mechanical properties in hot working. It should be noted that the addition of particles can induce extra strengthening of composites through dislocation strengthening and finer grains strengthening[9]. Moreover, the reinforcements also have dual effects on the DRX process of composites. On the one hand, particles can hinder the movement of grain boundary and restrict the growth of recrystallized grains. On the other hand, particles in soft matrix can act as potential sites for nucleation of recrystallization and increase the volume fraction of DRX[10]. As a consequence, it is significant

Received date: November 25, 2016
Foundation item: National Natural Science Foundation of China (51205028)
Corresponding author: Liu Shengpu, Candidate for Ph. D., General Research Institute of Nonferrous Metals, Beijing 100088, P. R. China, E-mail: lspcailiao@126.com

to understand the dynamic recrystallization behavior of composite for the optimal processing parameters and predict the critical conditions of DRX for composite precisely.

The conventional method used to determine the initiation of DRX for metals or alloys is the metallographic observation, which requires too much workload. An advanced approach based on strain hardening rate (θ) theory was adopted by Poliak and Jonas[11,12], and Ryan and McQueen[13]. They pointed that the peak stress (σ_p) corresponded to the point at which strain hardening rate was zero (θ=0) in the curves of θ-σ and the inflection point of θ-σ curves represented the critical stress. Furthermore, Najafizadeh and Jonas[14] simplified this method by fitting the θ-σ curves with a third order polynomial equation. Liu[15] calculated the exact values of critical stresses by taking the second derivative of θ-σ curves, where $d^2\theta/d^2\sigma$=0. So far, several studies have been conducted to predict the initiation of DRX for various metals or alloys, such as 42CrMo steel[16], 20MnNiMo steel[6], nickel-based superalloy[17], 7075 aluminum alloy[18], and AZ31B magnesium alloy[15]. There are also some attempts on DRX behavior of composites. Sun et al.[19] investigated the initiation and evolution of DRX for 30% SiC/Al composite using the process variables derived from flow curves and developed the DRX kinetics equations. Ko et al[20] predicted the dynamic recrystallization condition for SiC/2024Al composite by deformation efficiency. Yoo[21] developed the DRX model of SiC_w/AA2124 composites and obtained the grain size model in terms of temperature compensated strain rate. However, there were no any surveys on DRX characteristic of B_4C_p/Al composites.

The 6061Al alloy is an outstanding candidate for matrix of the metal matrix composite industrial applications due to its ideal mechanical properties. In the present work, the flow behavior of B_4C_p/6061Al composite at different deformation temperatures and strain rates has been analyzed to determine the critical conditions based on the strain hardening rate method. Furthermore, the DRX diagram of the composite has been established.

1 Experiment

The B_4C_p/6061Al composite used in this investigation contained 25 vol% B_4C particles with the average size of 5 μm, which was produced by PM (power metallurgy) route. The mass percentage of individual elemental alloy power of 6061Al alloy is shown in Table 1.

The samples with height of 15 mm and diameter of 10 mm were prepared. Graphite lubricant was used to minimize the friction between the dies and specimens. Isothermal hot compression tests were carried out on the Gleeble-1500 thermal simulator at temperatures ranging from 350 to 500 ℃ at an interval of 50 ℃ and the strain rate ranging from 0.001 to 1 s^{-1}. Each specimen was heated to the deformation temperature at a rate of 10 ℃/s, and held for 180 s at isothermal condition before compressing. Then the specimens were compressed to 50% reduction. Finally, at the end of compression the specimens were immediately quenched in water to reserve the deformed microstructure.

Table 1 Composition of 6061Al alloy (wt%)

Mg	Si	Cu	Fe	Cr	Mn	Ti	Al
0.89	0.65	0.25	0.25	0.075	0.03	0.02	Bal.

2 Results and Discussion

2.1 Analysis of stress-strain curves

The influence of different deformation temperatures and strain rates on the flow behavior of 25vol.% B_4C_p/6061Al composite is shown in Fig.1. According to the characteristics of stress-strain curves, the composite undergoes greater work hardening at a very small strain especially at lower temperatures (350 and 400 ℃) and higher strain rates (1 and 0.1 s^{-1}) because there is no enough time for energy accumulation and lower grain boundaries mobility. In other words, the dynamic softening during this stage is too weak to counteract the effects of strain hardening. With the increase of strain, the effect of softening is enhanced due to the occurrence of DRX. The flow stress increases up to a peak stress and then decreases until it reached a steady state. The steady stage is more obvious at higher temperatures (450 and 500 ℃) and lower strain rates (0.001 and 0.01s^{-1}). The occurrence of steady state means a new balance between softening and strain hardening is achieved.

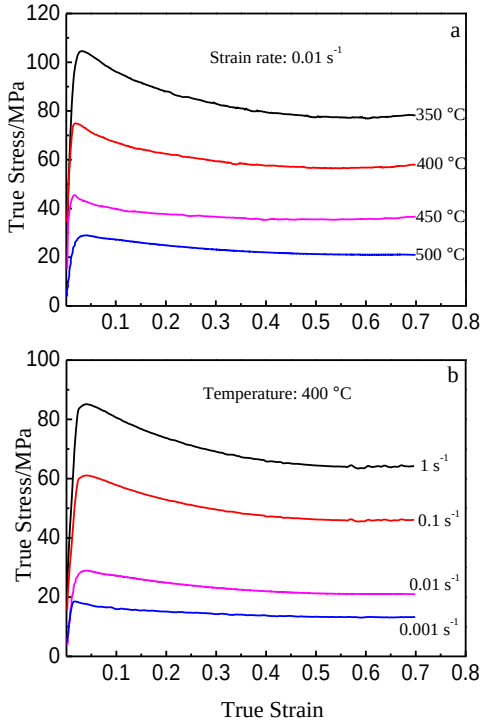

Fig.1 Flow stress curves of 25 vol% B_4C_p/6061Al composite: (a) $\dot{\varepsilon}$ =0.01 s^{-1} and (b) T=400 ℃

2.2 Constitutive equation for flow behavior of 25vol% B_4C_p/6061Al composite

For a given material, the relationship between the flow behavior and deformation conditions can be represented by an Arrhenius-type constitutive equation as follows[22]:

$$\dot{\varepsilon} = Af(\sigma)\exp(-Q/RT) \quad (1)$$

$$Z = \begin{cases} A_1\sigma^{n_1} = \dot{\varepsilon}\exp(Q/RT), & \alpha\sigma < 0.8 \\ A_2\exp(\beta\sigma) = \dot{\varepsilon}\exp(Q/RT), & \alpha\sigma > 1.2 \\ A[\sinh(\alpha\sigma)]^n = \dot{\varepsilon}\exp(Q/RT), & \text{for all} \end{cases} \quad (2)$$

Where, $\dot{\varepsilon}$ is strain rate, Q is the activation energy (kJ mol^{-1}); R is the gas constant (8.314 J (mol K)$^{-1}$; T is the absolute temperature (K); A is the structure factor (s^{-1}); α is stress level parameter (MPa^{-1}); n is stress exponent; A_1, A_2, A, n_1, n, α and β are the material constants, and $\alpha=\beta/n_1$.

The influence of strain rate and temperature on flow behavior can be described by the Zener-Hollomon parameter[23]:

$$Z = \dot{\varepsilon}\exp(Q/RT) \quad (3)$$

The peak stresses under different deformation conditions were used to evaluate the material constants. Taking the logarithm of Eq.(2), the following equations can be obtained:

$$\ln\dot{\varepsilon} = n_1\ln\sigma + \ln A_1 - Q/RT \quad (4)$$

$$\ln\dot{\varepsilon} = \beta\sigma + \ln A_2 - Q/RT \quad (5)$$

The values of n_1 and β can be easily obtained from the slope of $\ln\dot{\varepsilon}$-lnσ and $\ln\dot{\varepsilon}$-σ plots as shown in Fig.2, which are based on Eq.(4) and Eq.(5). The results are listed as follows: β=0.0938, n_1=7.8841, α=0.0119.

For all the stress levels, Eq.(1) and Eq.(3) can be represented as follows:

$$\dot{\varepsilon} = A[\sinh(\alpha\sigma)]^n \exp(-Q/RT) \quad (6)$$

$$Z = \dot{\varepsilon}\exp(Q/RT) = A[\sinh(\alpha\sigma)]^n \quad (7)$$

Taking the logarithm of both sides of Eq. (6) and the following equation can be gained:

$$\ln\dot{\varepsilon} = n\ln[\sinh(\alpha\sigma)] + \ln A - Q/RT \quad (8)$$

For the given strain rate, the deformation activation energy Q can be obtained by differentiating Eq. (8):

$$Q = Rn\left\{\frac{\partial\ln[\sinh(\alpha\sigma)]}{\partial(1/T)}\right\}_{\dot{\varepsilon}} \quad (9)$$

The plots of $\ln\dot{\varepsilon}$-ln[sinh($\alpha\sigma$)] and ln[sinh($\alpha\sigma$)]-1000/T can be obtained by substituting the values of flow stress, deformation temperature and corresponding strain rate into Eq.(9), as shown in Fig.3a and Fig.3b. Thus the value of Q can be evaluated as 206.149 kJ mol^{-1}.

By substituting the values of Q, $\dot{\varepsilon}$ and T into Eq.(7), the value of Z at different deformation conditions can be calculated.

Then taking the logarithm of both sides of Eq.(7), ln$Z$ can be represented as follows:

$$\ln Z = \ln A + n\ln[\sinh(\alpha\sigma)] \quad (10)$$

The relationship between ln$Z$ and ln[sinh($\alpha\sigma$)] can be seen in Fig.4. Obviously, it is better fitted. The value of n and ln$A$ is

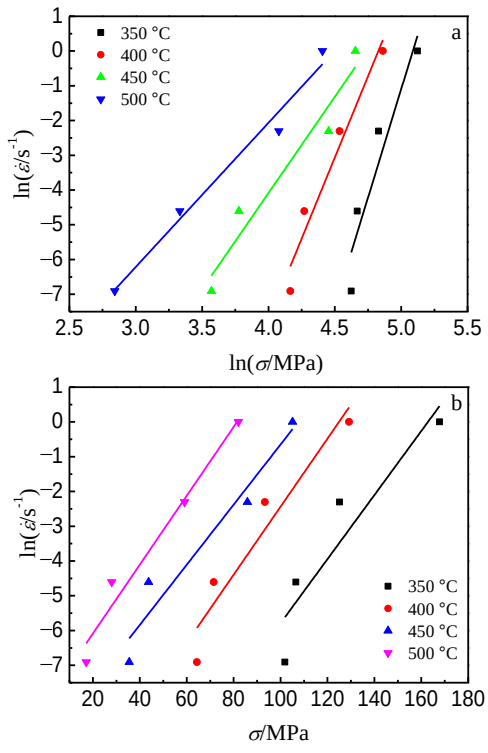

Fig.2 Relationship between strain rate and flow stress: (a) $\ln\dot{\varepsilon}$-lnσ and (b) $\ln\dot{\varepsilon}$-σ

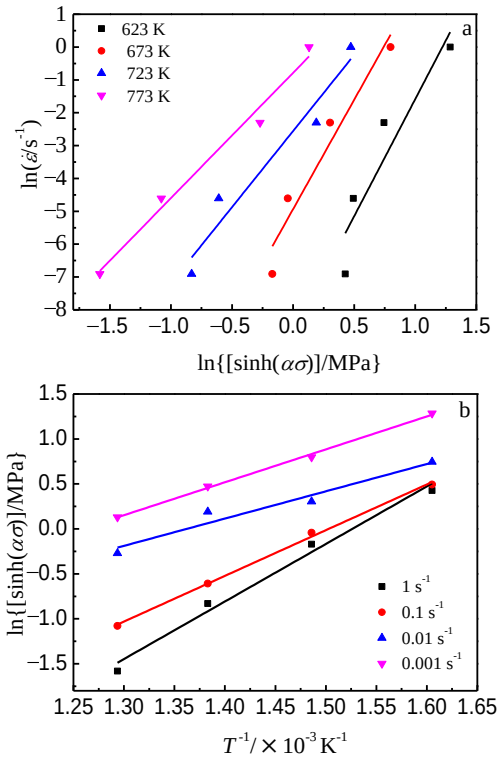

Fig.3 Relationships between flow stress with strain rate and temperature: (a) $\ln\dot{\varepsilon}$-ln[sinh($\alpha\sigma$)] and (b) ln[sinh($\alpha\sigma$)]-1000/T

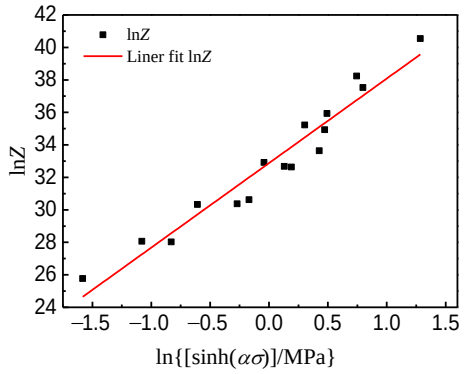

Fig.4 Relationships between ln$Z$ and ln[sinh($\alpha\sigma$)]

the slope and the intercept of ln$Z$-ln[sinh($\alpha\sigma$)] plot, respectively. Thus the value of A and n can be calculated as 3.13×10^{13} s^{-1} and 5.03, respectively. Finally, the constitutive equation of 25vol.% B_4C_p/6061Al composite is represented as Eq.(11).

$$\dot{\varepsilon}=3.13\times10^{13}\left[\sinh\left(0.0119\sigma\right)\right]^{5.03}\exp\left(-206.149/RT\right) \quad (11)$$

2.3 Critical conditions for DRX

The true stress-true strain curves shown in Fig.1 were used to calculate the values of strain hardening rate (θ=dσ/dε). Since the critical strain (ε_c) is lower than peak strain (ε_p), the stress values ranging from zero to peak stress (σ_p) were employed.

As shown in Fig.5, the θ was plotted as a function of σ for 500 ℃ and 0.001 s^{-1}. The inflection point of θ-σ curve was considered as the initiation of DRX. According to Najafizadeh and Jonas, the inflection point was detected by fitting a third order polynomial to the θ-σ curve as follows:

$$\theta=A\sigma^3+B\sigma^2+C\sigma+D \quad (12)$$

Where A, B, C and D are constants. Then the second derivative of Eq.(12) with respect to σ can be described as :

$$\frac{\mathrm{d}^2\theta}{\mathrm{d}^2\sigma}=6A\sigma^2+2B\sigma \quad (13)$$

When the Eq.(13) equals zero, the critical stress (σ_c) can be obtained. Thus,

$$6A\sigma_c+2B=0\Rightarrow\sigma_c=-B/3A \quad (14)$$

The third order polynomial fitted θ-σ curves correspond to the red dash lines in Fig.5. It is clear that, the 3rd curves agree well with original curves. Therefore, this method can be used to calculate the critical stress for initiation of DRX precisely. Then, the critical strain can be determined back into stress-strain curves in Fig.1. The whole calculated critical conditions for 25 vol% B_4C_p/6061Al composite are listed in Table 2.

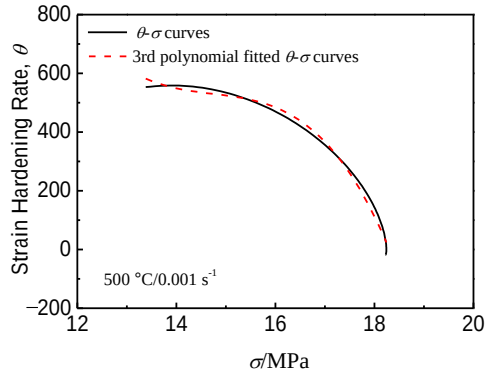

Fig.5 θ-σ curves of 25 vol% B_4C_p/6061Al composite at 500 ℃/0.001 s^{-1}

It can be observed that the critical stress (σ_c) and critical strain (ε_c) change with temperature and strain rate irregularly. It is calculated that $\varepsilon_c/\varepsilon_p$ = 0.49–0.89, σ_c/σ_p = 0.08–0.64, and there is a liner relationship between σ_c and σ_p as shown in Fig.6.

In order to describe the effect of the deformation conditions on the critical conditions for DRX, the Zener-Hollomon parameter was introduced. Based on Sellars model[19], the critical strains are usually shown as power-law functions of Z:

$$\varepsilon_c=aZ^b \quad (15)$$

Where a and b are constants. The relationship between natural logarithm of critical strain and natural logarithm of the Z

Table 2 Critical values of 25 vol% B_4C_p/6061Al composite under different deformation conditions

Temperature/℃	Strain rate/s^{-1}	σ_c/MPa	σ_p/MPa	ε_c	ε_p
350	0.001	90.8193	101.87	0.0129	0.0248
	0.01	88.1391	106.57	0.0136	0.0330
	0.1	105.3566	125.15	0.0152	0.0422
	1	134.4074	167.76	0.0191	0.0480
400	0.001	58.5768	67.344	0.0089	0.0213
	0.01	64.1275	74.919	0.0088	0.0246
	0.1	78.8007	97.451	0.0099	0.0312
	1	122.7327	140.67	0.0167	0.0406
450	0.001	29.2667	35.5269	0.0068	0.0173
	0.01	33.3084	43.7258	0.0050	0.0170
	0.1	69.9053	85.8651	0.0059	0.0311
	1	88.7761	105.1387	0.0146	0.0355
500	0.001	14.7259	19.678	0.0046	0.0360
	0.01	25.1355	28.0229	0.0037	0.0227
	0.1	48.4238	59.0776	0.0022	0.0261
	1	64.9323	82.0281	0.0028	0.0278

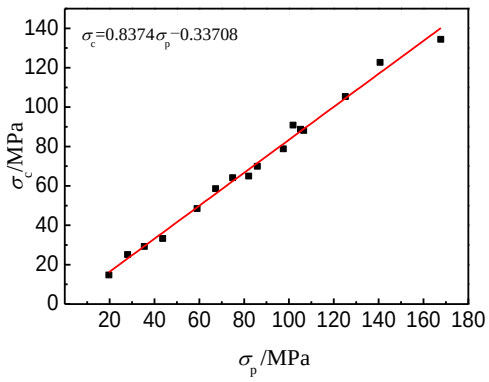

Fig.6 Relationship between critical stress (σ_c) and peak stress (σ_p)

parameter is shown in Fig.7, which reveals an approximated liner relationship.

Thus, the equation for critical strain as a function of Z can be easily obtained:

$$\varepsilon_c = 2.39\times10^{-4} Z^{0.11022} \quad (16)$$

2.4 DRX diagram of 25 vol% B_4C_p/6061Al composite

DRX diagram can contribute to a better understanding of the whole DRX process, which contains both critical strain and steady-state strain. The steady-state strain (ε_{ss}) can be identified by the plot of strain hardening rate with strain (θ-ε). The second point at which the strain hardening rate equals zero corresponds to the initiation of steady-state strain. The θ-ε curves under different strain rates at 500 ℃ is shown in Fig.8.

Table 3 gives the values of steady-state strain (ε_{ss}) at various deformation conditions.

Accordingly, DRX diagrams of 25 vol% B_4C_p/6061Al composite can be obtained (Fig.9)

It is clear that ε_c and ε_{ss} divide the whole deformation process into three parts: non-DRX zone, partly-DRX zone and completely-DRX zone. Moreover, both the ε_c and ε_{ss} increase with the increase of Z and the values of ε_{ss} mainly converge on 0.5.

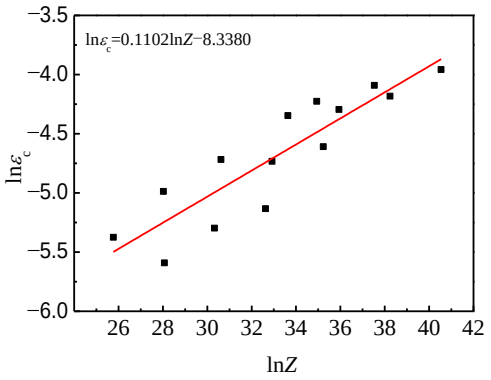

Fig.7 Relationship between critical strain lnε_c and ln$Z$

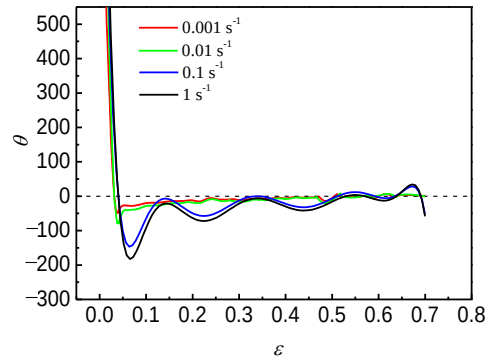

Fig.8 Relationship between strain hardening rate (θ) and strain (ε) under different strain rates at 500 ℃

Table 3 Steady-state strain (ε_{ss}) of 25 vol% B_4C_p/6061Al composite under different deformation conditions

Strain rate/ s^{-1}	Temperature/ ℃			
	350	400	450	500
0.001	0.5194	0.5261	0.5056	0.5048
0.01	0.5145	0.5267	0.4920	0.5103
0.1	0.5147	0.5336	0.5072	0.5131
1	0.5152	0.5332	0.5148	0.5274

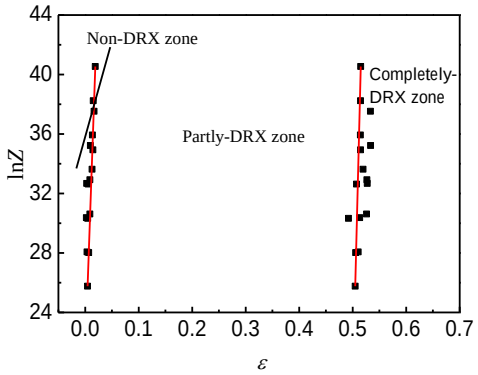

Fig.9 DRX diagrams of 25 vol% B_4C_p/6061Al composite

3 Conclusions

1) The flow behavior of the 25vol% B_4C_p/6061Al composite is sensitive to deformation temperature and strain rate. An Arrhenius type constitutive equation is developed using the peak stress in the range of deformation temperatures from 350 to 500 ℃ and strain rates from 0.001 to 1 s^{-1} as follows:

$$\dot{\varepsilon} = 3.13\times10^{13}\left[\sinh(0.0119\sigma)\right]^{5.03}\exp(-206.149/RT)$$

2) The main softening mechanism of 25 vol% B_4C_p/6061Al composite is dynamic recrystallization. Based on the strain hardening rate method, the critical strain for initiation of DRX can be obtained from the inflection point on the θ-σ curves and the critical stress (σ_c) can be determined back into stress-strain curves. There is a liner relationship between critical stress and peak stress, and the critical strain can be described by Z parameter as follows: $\varepsilon_c=2.39\times10^{-4}Z^{0.11022}$.

3) The steady-state strains can be obtained through θ-ε curves and the DRX diagram is established. The values of ε_{ss} mainly converge on 0.5.

References

1 Wu C, Fang P, Luo G *et al*. *Journal of Alloys & Compounds*[J], 2014, 615(2): 276

2 Alizadeh M, Paydar M H. *Materials Science & Engineering A*[J], 2012, 538(11): 14

3 Xu Z G, Jiang L T, Zhang Q *et al*. *Materials & Design*[J], 2016, 111: 375

4 Chen H S, Wang W X, Li Y L *et al*. *Materials & Design*[J], 2016,

94: 360
5 Gangolu S, Rao A G, Sabirov I *et al*. *Materials Science & Engineering A*[J], 2016, 655: 256
6 Wang M H, Li Y F, Wang W H *et al*. *Materials & Design*[J], 2013, 45: 384
7 Wei H L, Liu G Q, Xiao X *et al*. *Materials Science & Engineering A*[J], 2013, 573(3): 215
8 Mirzadeh H, Najafizadeh A. *Materials & Design*[J], 2010, 31(3): 1174
9 Srivastava V C, Jindal V, Uhlenwinkel V *et al*. *Materials Science and Engineering: A*[J], 2008, 477(1): 86
10 Ferry M, Munroe P R. *Composites Part A: Applied Science and Manufacturing*[J], 2004, 35(9): 1017
11 Poliak E I, Jonas J J. *ISIJ international*[J], 2003, 43(5): 684
12 Jonas J J, Poliak E I. *Materials Science Forum*[J], 2003, 426(1): 57
13 Ryan N D, McQueen H J. *Can Metall Q*[J], 1990, 29(2) : 147
14 Mirzadeh H, Najafizadeh A. *Materials & Design*[J], 2010, 31(3): 1174
15 Liu J, Cui Z, Ruan L. *Materials Science and Engineering A*[J], 2011, 529: 300
16 Quan G Z, Li G S, Chen *et al*. *Materials Science & Engineering A*[J], 2011, 528(13-14):4643
17 Chen X M, Lin Y C, Wen D X *et al*. *Materials & Design*[J], 2014, 57(5): 568
18 Quan G Z, Mao Y P, Li G S *et al*. *Computational Materials Science*[J], 2012, 55: 65
19 Sun Y, Xie J, Hao S *et al*. *Journal of Alloys & Compounds*[J], 2015, 649: 865
20 Ko B C, Yoo Y C. *Journal of Materials Science*[J], 2000, 35(16): 4077
21 Yoo Y C, Jeon J S, Ko B C. *Materials Science Forum*[J], 1996, 217-222 :1157
22 Sellars C M, Mctegart W J. *Acta Metallurgica*[J], 1966, 14(9): 1136
23 Zener C, Hollomon H. *Journal of Applied Physics*[J], 1946, 17(2): 69

B_4C_p/6061Al 复合材料动态再结晶临界条件

刘生璞，李德富，郭胜利
(北京有色金属研究总院，北京 100088)

摘　要：通过等温热压缩实验对 25% B_4C_p/6061Al（体积分数）复合材料的热变形行为和动态再结晶临界条件进行了研究，采用的温度范围为 350~500 ℃，应变速率范围为 0.001~1 s^{-1}。应力-应变曲线显示动态再结晶是复合材料热变形过程中主要的软化机制，并采用峰值应力构建了基于 Arrhenius 形式的本构方程。基于加工硬化率曲线，求解了表示动态再结晶发生的临界应变与临界应力值。结果表明，临界应力与峰值应力存在线性关系：σ_c=0.8374σ_p–0.33708。此外，引入 Zener-Hollomon 参数描述变形条件对临界条件的影响，得到临界应变与 Z 参数的关系：ε_c=2.39×$10^{-4}Z^{0.11022}$。最后，通过 θ-ε 曲线得到了复合材料完成动态再结晶时的稳态应变，并绘制了动态再结晶图。

关键词：B_4C_p/6061Al 复合材料；动态再结晶；临界条件；加工硬化率

作者简介：刘生璞，男，1992 年生，博士生，北京有色金属研究总院，北京 100088，E-mail: lspcailiao@126.com